IOPscience iopscience.iop.org

Home Search Collections Journals About Contact us My IOPscience

Inhomogeneous electronic states in organic metal $(BEDO\text{-}TTF)_2ReO_4 \cdot H_2O$: EPR and SQUID study

This article has been downloaded from IOPscience. Please scroll down to see the full text article.

2007 J. Phys.: Condens. Matter 19 406210

(http://iopscience.iop.org/0953-8984/19/40/406210)

View the table of contents for this issue, or go to the journal homepage for more

Download details:
IP Address: 129.252.86.83
The article was downloaded on 29/05/2010 at 06:09

Please note that terms and conditions apply.

IOP PUBLISHING JOURNAL OF PHYSICS: CONDENSED MATTER

J. Phys.: Condens. Matter **19** (2007) 406210 (10pp) doi:10.1088/0953-8984/19/40/406210

Inhomogeneous electronic states in organic metal $(BEDO\text{-}TTF)_2ReO_4{\cdot}H_2O$: EPR and SQUID study

Yu N Shvachko[1], D V Starichenko[1], A V Korolyov[1], N D Kushch[2] and E B Yagubskii[2]

[1] Institute of Metal Physics, Ural Division of Russian Academy of Sciences, Ekaterinburg, Russian Federation
[2] Institute of Problems of Chemical Physics, Russian Academy of Sciences, Chernogolovka, Russian Federation

E-mail: yurii.shvachko@imp.uran.ru

Received 18 May 2007, in final form 21 May 2007
Published 11 September 2007
Online at stacks.iop.org/JPhysCM/19/406210

Abstract

It is shown by electron paramagnetic resonance (EPR) and superconducting quantum interference device (SQUID) magnetometry that two spin systems coexist in conducting layers of the quasi-2D organic metal $(BEDO\text{-}TTF)_2ReO_4{\cdot}H_2O$: delocalized moments of charge carriers (holes), $I_{epr}(300\ K) = 1.62 \times 10^{-4}$ emu mol^{-1}, and localized moments on $BEDO\text{-}TTF^{+1}$, $\chi_p(300\ K) = 4.25 \times 10^{-4}$ emu mol^{-1}. The phase transition Me–Me′ at $T_c = 203$ K is detected in paramagnetic relaxation, EPR amplitude and resistivity. Magnetic susceptibilities, I_{epr} and χ_p, are not sensitive to the transition. Due to fine rearrangement of ReO_4 linked by H_2O, the electronic spectrum becomes inhomogeneous. Below the transition exchange-coupled localized states within the metallic phase are observed. On cooling, the concentration of delocalized moments gradually decreases, contributing to a localized spin system. The phenomenon is interpreted in terms of short-range antiferromagnetic (AFM) interactions via conducting electrons. Below 14 K the AFM coupled states decay, and paramagnetism of local moments is recovered.

1. Introduction

Charge-transfer complexes based on the BEDT-TTF (ET) (bis(ethylenedithio) tetrathiafulvalene) donor molecule and its derivative, BEDO-TTF (bis(ethylenedioxy) tetrathiafulvalene), demonstrate a great variety of crystal structures with two-dimensional (2D) conducting sheets alternating with insulating anion layers [1, 2]. The conducting plane consists of stacks of cation radicals with their long axes being nearly perpendicular to the plane. Due to their spatial proximity, the molecular orbitals of sulfur hetero atoms substantially overlap, forming a π-type conduction band. Charge transfer induces partial filling of the band, which allows the

hopping of holes within the layer and metallic behavior at half filling. The electric properties of ET-based materials with inorganic tetrahedral, octahedral and polyhedral anions ($InBr_4$, $CuBr_4$, BrO_4, GaI_4, InI_4, AsF_6, SbF_6, PF_6, etc) are characterized by metal–insulator (Me–I) transitions at high temperatures 90–300 K [1]. In most compounds the order–disorder transitions in anion layers are responsible for drastic changes of transport properties. Thus, these materials can be considered as 'organic–inorganic molecular composites' or 'chemically constructed multilayers' [3]. The charge-transfer salt (BEDO-TTF)$_2$ReO$_4$·H$_2$O is of particular interest due to unusual metal–metal′ (Me–Me′) phase transition.

Microscopic inhomogeneous electronic states have attracted much attention recently in different kinds of correlated electron systems. Materials with intrinsic electronic inhomogeneity reveal critical phenomena in charge, spin, orbital, and lattice degrees of freedom. Their magnetic properties are nontrivial. The family of organic conductors based on the BEDT-TTF molecule and its derivatives such as BEDO-TTF belongs to the highly correlated electron systems. Among them the organic conductors (BEDO-TTF)$_2$X exhibit bandwidth-controlled Mott quasi-electronic spectra, in contrast to the filling-controlled one in inorganic perovskites, such as high-T_c copper oxides. Therefore, an intrinsic electronic inhomogeneity is expected to appear in the vicinity of the phase transition in (BEDO-TTF)$_2$X.

In a series of earlier works, the transport and magnetotransport properties of (BEDO-TTF)$_2$ReO$_4$·H$_2$O were intensively studied [4–9]. However, most of the studies dealt with helium temperatures and the superconducting transition. Unusual magnetic properties below 213 K were first observed by EPR and interpreted in terms of a spin-density-wave (SDW) state below the phase transition Me–Me′ [6]. However, this interpretation was not consistent with later direct x-ray experiments [8]. Thus, the problem of the low-temperature magnetic state has remained open.

By using magnetic and resonance methods we have studied the evolution of the electronic spectrum of (BEDO-TTF)$_2$ReO$_4$·H$_2$O in accordance with the Me–Me′ phase transition. The work has also been stimulated by the recent observation of a new phenomenon of the coexistence of localized and delocalized electronic states in the related system (BET-TTF)$_2$ReO$_4$ [10].

2. Experimental details

The crystals of (BEDO-TTF)$_2$ReO$_4$·H$_2$O were synthesized by electrochemical oxidation of BEDO-TTF in 1,2-dichloroethane-ethanol (10 vol%) medium in the constant current regime, $I = 0.3$ μA, at $T = 293$ K. (Bu$_4$N)ReO$_4$ salt was used as an electrolyte [4]. The black shiny crystals with the plate-like shape were grown on a platinum electrode within 1–2 weeks. Typical sizes of the single crystals were $(1 \times 0.3 \times 0.03)$ mm^3.

The charge-transfer salt (BEDO-TTF)$_2$ReO$_4$·H$_2$O has a layered structure of β'-type with cation-radical layers (ab plane) and insulating anion sheets alternating along the c-axis. The b-axis is directed perpendicularly to C=C bond in the plane of the BEDO-TTF molecule. The cation radicals BEDO-TTF$^{+1/2}$ form conducting layers through the 2D network of short S $\cdots$ S (3.346–3.661 Å) and S $\cdots$ O (3.152–3.208 Å) contacts [4, 8, 9]. The anion layer consists of the ReO_4 tetrahedral anions and water molecules. Due to hydrogen bonds, H_2O molecules stabilize the packing of ReO_4 anions. At room temperature the hydrogen bonds are formed between an H_2O molecule and only one ReO_4 anion. The length of this bond is 2.59 Å. At low temperatures ($T < 200$ K), a reorientation of ReO_4 takes place. Here the neighboring tetrahedra are linked via solvent molecules. Each H_2O molecule is now homogeneously bound with two oxygen atoms of ReO_4 neighbors. It is likely that polymeric chains are formed. Detailed analysis of the crystals and band structures has been performed earlier [4, 8]. Resistivity measurements at low temperatures have also been performed [4].

The standard CW X-band EPR method was used to study magnetic and relaxation properties at $100 < T < 350$ K (nitrogen gas flow cryostat). A set of small crystals was placed on a mica substrate in the TE_{102} cavity. The MW power level was kept as 2 mW. The EPR spectra (the first derivative of the absorption signal) were recorded at fixed points while cooling down slowly to 100 K, and then while heating of the sample up to 350 K with a typical rate 1–2 K min^{-1}. The signal intensity, I_{epr}, was determined by double integration (Schumacher–Slichter technique) of the EPR spectrum at a magnetic field sweep $\delta B_{sw} > 5\Delta B$, where ΔB is the peak-to-peak EPR linewidth [11]. For a single Lorentz EPR line this procedure gives ∼10% relative error. Absolute values of the integrated intensity, I_{epr}, and g-factor were calibrated by using a coal-pitch probe and $CuSO_4{\cdot}5H_2O$.

The complete response, $\chi_p(T)$, and magnetization, $M(B)$, were directly measured by using a Quantum Design MPMS SQUID magnetometer. Randomly oriented $(BEDO\text{-}TTF)_2ReO_4{\cdot}H_2O$ powder was put on a mica substrate oriented perpendicularly to B_0. A typical specimen used for measurement weighed 5–15 mg. The diamagnetic contribution of the mica substrate measured at 300 K was less than 1% of the paramagnetic signal. The diamagnetic response was subtracted from the basic SQUID signal over the entire temperature range. The Pascal diamagnetic contribution for BEDO-TTF, -2.6×10^{-4} emu mol^{-1}, was also taken into consideration. The $\chi_p(T)$ measurements were carried out on cooling from 300 K down to 2 K in an external magnetic field $B_0 = 1$ T. Within the interval $160 < T < 240$ K, $\chi_p(T)$ was also repeatedly measured under a temperature cycling regime at the rate 1 K min^{-1}. The $M(B)$ dependence was measured up to 5 T.

Since the spin contributions to magnetic susceptibility were determined independently by EPR, $I_{epr}(T)$ and by the SQUID, $\chi_p(T)$ (below in the text), the behavior of the spin contribution, χ_s, extracted from the magnetic resonance is discussed in terms of EPR signal intensity I_{epr} ($\chi_s \sim I_{epr}$).

3. Results

A symmetric EPR signal with $g = 2.014$–2.015 is observed within the studied temperature range, 100–300 K. The EPR linewidth $\Delta B(300\ \text{K}) = 45$ G is typical for (BEDT-TTF)-based organic conductors [1]. This signal can be definitely attributed to the cation-radical layer. However, the identification of the electronic states of BEDO-TTF responsible for this signal requires more detailed analysis. The absence of additional EPR signals with hyperfine structure (HFS) typical for Re^{4+} (^{185}Re, ^{187}Re isotopes) indicates that all the Re cations are diamagnetic, i.e. we have Re^{7+} with $5d^0$ configuration. A comparison of the temperature evolution of the EPR linewidth, $\Delta B(T)$, and dc resistivity, $\rho(T)$, in $(BEDO\text{-}TTF)_2ReO_4{\cdot}H_2O$ is shown in figure 1. As $\rho(T)$ reveals metallic behavior, $\Delta B(T)$ also gradually narrows on cooling, which is qualitatively consistent. Even though the plot margin is 93 K, the metallic behavior of resistivity is observed down to 4.2 K, where $\rho(4.2\ \text{K}) = 0.003\ \Omega$ cm.

In the vicinity of $T = 203$ K both the parameters undergo abrupt changes: the resistivity drops from 0.021 to 0.014 Ω cm, which is ∼30%, and the linewidth increases from 32.3 to 36.3 G, which is ∼12%. These changes agree fairly well with an earlier reported first-order structural transition [8]. Hence, the influence of structure changes on the magnetic and transport properties can be interpreted in terms of an electronic phase transition. Meanwhile, the broadening of the EPR signal and the character of the transition disagree with earlier published EPR data [6]. The temperature evolution of both $\Delta B(T)$ and $\rho(T)$ has irreversible behavior (hysteresis) on cooling and heating. This behavior is in good agreement with the hysteretic behavior of the (080) reflection intensity in the x-ray spectra [8]. The width of thermal hysteresis for $\Delta B(T)$ is $\Delta T = 12$ K, giving the estimate of transition temperature

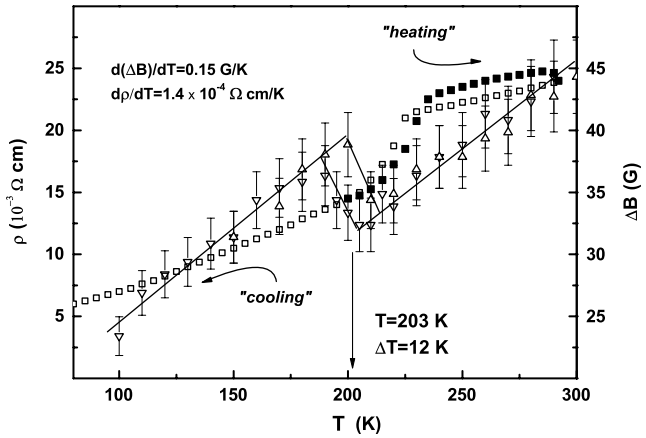

Figure 1. Temperature dependences of EPR linewidth, $\Delta B(T)$, on heating ($\triangle$) and cooling ($\triangledown$) and corresponding dc resistivity, $\rho(T)$ ($\blacksquare$, $\square$), ($\rho(300\ \mathrm{K}) \approx 0.025\ \Omega$ cm) for (BEDO-TTF)$_2$ReO$_4$·H$_2$O. Solid lines with $\mathrm{d}(\Delta B(T))/\mathrm{d}T = 0.15\ \mathrm{G\ K^{-1}}$ are the best fit for ranges $100 < T < 203$ K and $203 < T < 300$ K. Within the interval $197 < T < 209$ K, ΔB shows hysteretic behavior. The resistivity demonstrates hysteretic behavior at $T > 208$ K. Below the transition $\rho(T)$ is proportional to the temperature with $\mathrm{d}\rho(T)/\mathrm{d}T = 1.4 \times 10^{-4}\ \Omega\ \mathrm{cm\ K^{-1}}$ down to 4.2 K.

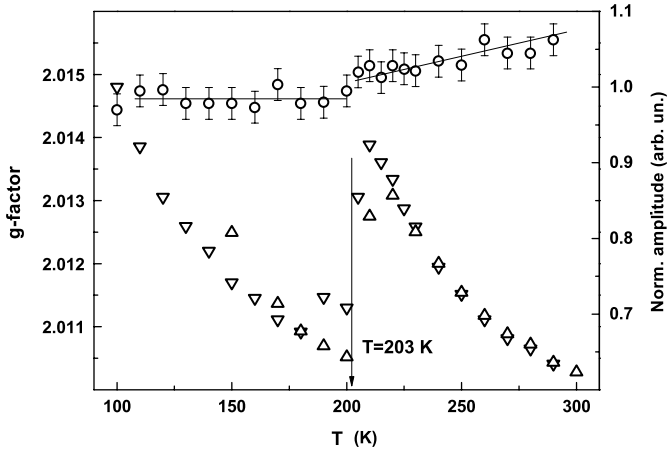

Figure 2. Temperature dependences of g-factor ($\circ$) and normalized amplitude of the EPR signal in the cooling ($\triangledown$) and heating ($\triangle$) regimes for (BEDO-TTF)$_2$ReO$_4$·H$_2$O. The solid lines are linear approximations.

$T = 203$ K. The linewidth, $\Delta B(T)$, is proportional to the temperature with the same coefficient $\mathrm{d}(\Delta B(T))/\mathrm{d}T = 0.15\ \mathrm{G\ K^{-1}}$ for $100 < T < 203$ K and $203 < T < 300$ K segments (see fitting lines in figure 1). The resistivity shows a pronounced slope with $\mathrm{d}\rho(T)/\mathrm{d}T = 1.4 \times 10^{-4}\ \Omega\ \mathrm{cm\ K^{-1}}$ below 210 K. The transition takes place at $T = 223$ K (half-width).

The temperature dependence of the g-factor shown in figure 2 also indicates the transition at 203 K, although revealing negligible change $\Delta g = 0.0004$ near the transition. At $T < 203$ K, the g-factor is temperature independent, and it increases slightly at $T > 203$ K (see fitting lines in figure 2). The absolute values $g(293\ \mathrm{K}) = 2.015(6)$ and $g(103\ \mathrm{K}) = 2.014(4)$ are close to the g-factor of free electrons, which is typical for conduction electron spin

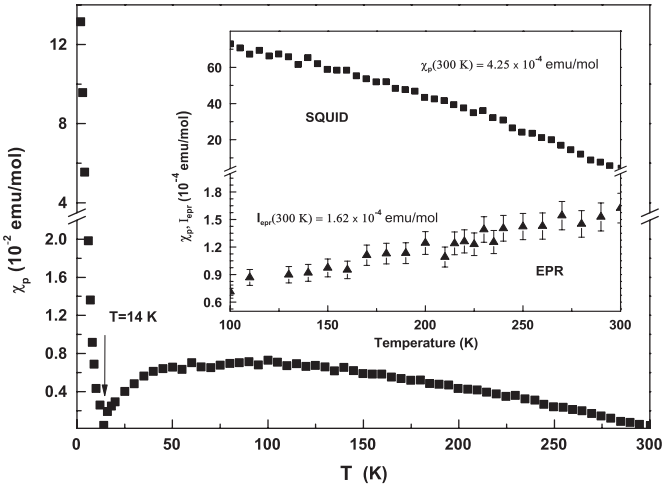

Figure 3. Temperature dependence of paramagnetic susceptibility, $\chi_p(T)$, for (BEDO-TTF)$_2$ReO$_4$·H$_2$O. The inset shows high-temperature segments of $\chi_p(T)$ (■) and double integrated EPR intensity, $I_{epr}(T)$ (▲). At room temperature $\chi_p = 4.25 \times 10^{-4}$ emu mol^{-1} and $I_{epr} = 1.62 \times 10^{-4}$ emu mol^{-1}.

resonance. The behavior of the EPR linewidth and g-factor is consistent with a metallic state above and below the transition temperature $T = 203$ K. Thus, the EPR signal in the crystals studied is attributed to conduction electrons (holes).

In figure 2 we also plot the normalized amplitude of the EPR signal in the cooling (▽) and heating (△) regimes. The experimental points clearly indicate the transition temperature at 203 K.

The spin contribution to the magnetic susceptibility obtained from the EPR spectra, $I_{epr}(T)$, is shown in figure 3 (see inset). At 300 K, I_{epr} contributes 1.62×10^{-4} emu mol^{-1}. In the range $100 < T < 300$ K the intensity decreases proportionally, by nearly two times. Although the amplitude of the EPR signal clearly reveals the transition (see figure 2), the intensity and, respectively, the spin susceptibility of conduction electrons (holes) do not show any changes at 203 K. This behavior contradicts earlier EPR results [6], where a drop of two times the EPR intensity was observed at 213 K. We believe that both the EPR results indicate incomplete response of the total spin ensemble. To confirm this, measurements of static magnetic susceptibility were carried out.

The solid squares in figure 3 denote the temperature dependence of the paramagnetic susceptibility, $\chi_p(T)$, measured by the SQUID. At 300 K, the absolute value of χ_p is 4.25×10^{-4} emu mol^{-1}. It increases up to 7.3×10^{-3} emu mol^{-1} at 100 K (see inset in figure 3). At $14 < T < 50$ K, χ_p decreases following the trend $\chi_p \to 0$; as $T \to 14$ K, $\chi_p(14\text{ K}) = 4.4 \times 10^{-4}$ emu mol^{-1} (see figure 3). Below 14 K χ_p recovers to 1.25×10^{-1} emu mol^{-1} at 2 K within $\Delta T = 12$ K. The paramagnetic susceptibility, χ_p, takes into account the total magnetic response of the whole spin ensemble. Therefore, (χ_p–I_{epr}) characterizes the localized spin states. Its value at 2 K is consistent with the Curie–Weiss estimate for the localized moments detected at room temperature. Both $I_{epr}(T)$ and $\chi_p(T)$ data are not sensitive to the transition at 203 K.

While $I_{epr}(T)$ reflects the evolution of a spin fraction of delocalized charge carriers (π-type holes), its temperature dependence can be attributed to the evolution of the density of

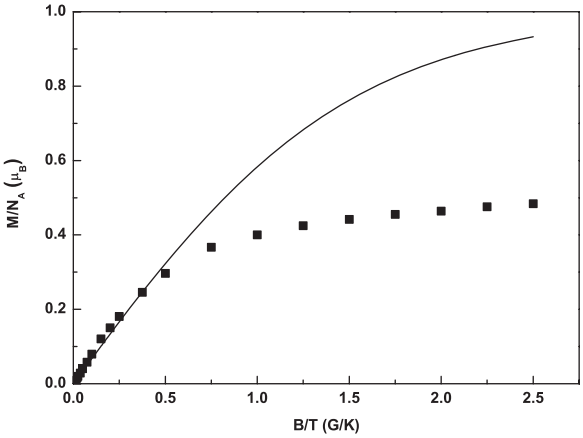

Figure 4. Field dependence of magnetization, $M(B)$, for (BEDO-TTF)$_2$ReO$_4$·H$_2$O at $T = 2$ K. The solid line is the Brillouin function for $S = 1/2$.

states (DOS) at the Fermi level, $n(\varepsilon_F)$:

$$I_{epr}(T) \sim n(\varepsilon_F)\mu_B^2. \tag{1}$$

The DOS calculated for the four highest occupied bands of a single donor molecule layer of (BEDO-TTF)$_2$ReO$_4$·H$_2$O has no maximum at ε_F, $n(\varepsilon_F) \sim 6$ DOS/(unit cell), which is relatively weak as compared to β-type metals [6]. So, the fraction of delocalized spins forms a minor Pauli contribution to $\chi_p(T)$. The linear temperature evolution of $I_{epr}(T)$ indicates that the DOS value at the Fermi level decreases by 50% while cooling from 300 to 100 K. The unit cell volume, V, determined from x-ray analysis also proportionally decreases from 2781.3 Å^3 at 293 K to 2710.(0) Å^3 at 140 K [8]. Hence, the temperature evolution of the EPR intensity at $100 < T < 300$ K cannot be explained by the compression of the unit cell.

The field dependence of magnetization, $M(B)$, measured at 2 K within 0–5 T, gives a curve resembling the Brillouin function for $S = 1/2$. In figure 4 the magnetization data are depicted in Bohr magneton units versus the normalized scale 'field/temperature', B/T ($T = 2$ K). However, the experimental points lie at lower values, ∼50%. This is in good agreement with $\chi_p(300\text{ K})$ giving approximately 20% of all spins in localized states. Besides that, the concentration of local moments increases with cooling. The contribution of conduction electrons is negligible.

Thus, the spins that have 'disappeared' for EPR still contribute as local moments to the paramagnetic susceptibility χ_p measured by the SQUID. The response of this fraction is dominant at low temperatures. These results are in agreement with the published Hall resistivity data [6]. Indeed, delocalized carriers are holes and localized moments are electrons.

Several individual platelet-like single crystals were mounted on a sample holder for detailed EPR measurements. The angular dependences of the resonance field, B_{res} (■), and signal linewidth, ΔB (□), at $T = 293$ K are depicted in figure 5. $B_{res}(\Theta)$ is well described in terms of axial anisotropy [12]:

$$B_{res}(\Theta) = (B_{res\|}^2 \cdot \cos^2\Theta + B_{res\perp}^2 \cdot \sin^2\Theta)^{1/2}, \tag{2}$$

where Θ is the angle between the external magnetic field B_0 and the conducting crystal plane ab. 0° and 90° correspond to parallel and perpendicular orientations of B_0 with $B_{res\|} = 3333$ G ($g_\| = 2.015(6)$) and $B_{res\perp} = 3346$ G ($g_\perp = 2.007(6)$). At 103 K the angular behavior remains unchanged and shifted with $B_{res\|} = 3334$ G and $B_{res\perp} = 3347$ G, respectively. The best fit for $\Delta B(\Theta)$ is given by the expression

$$\Delta B(\Theta) = \Delta B_0 + (\Delta B_\perp^2 \cdot \cos^2\Theta + \Delta B_\|^2 \cdot \sin^2\Theta)^{1/2} - \Delta B(1 - 3\cos^2\Theta)^{4/3}, \tag{3}$$

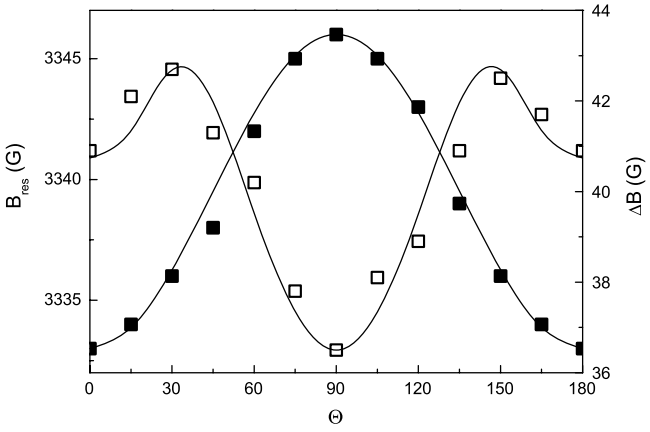

Figure 5. Angular dependences of resonance field, $B_{res}(\theta)$ (■), and EPR linewidth, $\Delta B(\theta)$ (□), for (BEDO-TTF)$_2$ReO$_4$·H$_2$O at $T = 293$ K. Solid lines are theoretical dependences from equations (2) and (3), respectively.

where $\Delta B_0 = 6.2$ G, $\Delta B = 2.5$ G, $\Delta B_\perp = 36.5$ G and $\Delta B_\parallel = 37$ G at $T = 293$ K. Solid lines for equations (2) and (3), respectively, are represented in figure 5. Note that the maximum value, $\Delta B = 42.7$ G, at $\Theta = 30°$ is in good agreement with the total linewidth for the powder sample, which indicates spin-lattice relaxation but not an inhomogeneous broadening. At $T = 103$ K the angular behavior does not change qualitatively.

4. Discussion

A metal–insulator transition at temperatures $T \geqslant 80$ K is a common feature for most of the BEDT-TTF-based charge-transfer salts with tetrahedral and octahedral anions [1]. Independently of the electronic band characteristics of the 2D S···S network, the transition shifts to higher temperatures as a polymeric chain (or solvent hydrogen bonds) forms a link between individual anions. For d-metal complexes in an anion sublattice the transition temperature may rise to ∼200 K, so the compound becomes a semiconductor at room temperature [13]. The salt (BEDO-TTF)$_2$ReO$_4$·H$_2$O demonstrates similar structural properties in the vicinity of 200 K. Meanwhile, it remains metallic below the transition due to weak participation of the oxygen p orbitals in the highest occupied molecular orbital (HOMO). Hence, the structural rearrangements of ReO$_4$ anions do not cause drastic changes of the quasi-electronic spectra.

Indeed, the network of hydrogen bonds in the anion layer and the absence of sulfur atoms in the outer rings of the BEDO-TTF molecule diminish the influence of anion reorientation on the band characteristics in comparison with BEDT-TTF. Partially this is owing to the fact that the sulfur atoms in inner rings are less sensitive to the order/disorder in the terminal ethylene groups of BEDO-TTF molecule. Note that (BEDT-TTF)$_2$ReO$_4$, which does not contain a H$_2$O 'bridge' between ReO$_4$, demonstrates a Me–I transition at 80–90 K [6].

The increase of ΔB (∼30%, figure 1) at $T \approx 203$ K correlates with the contraction of the cation-radical layer along the b-axis. However, the overall changes of transfer integrals are quite insensitive to the detected transformations in S···S and S···O short contacts [8]. Therefore, an additional contribution to spin-lattice relaxation is not likely to be attributed to the band characteristics. Even though the curve $g(\theta)$ is typical for conductors with axial anisotropy, the contribution $\sim(1 - 3\cos^2\theta)$ to $\Delta B(\theta)$ indicates the presence of an unexpected relaxation mechanism. Similar angular behavior was observed at 103 K. A traditional spin–phonon relaxation ($1/T_1$) mechanism is described by the Elliot expression [1]:

$$\Delta B = 1/\gamma T_1 = (\Delta g)^2 \tau^{-1} \tag{4}$$

and

$$\rho = (m/ne^2)\tau^{-1}, \tag{5}$$

where γ is the gyromagnetic ratio, $\Delta g = (g - 2.0023)$, τ^{-1} is a scattering rate of conduction electrons (holes), and n, e, m are the concentration, charge and effective mass of conduction electrons. Within the spin–phonon approach, ΔB and ρ have similar temperature behavior. The lower resistivity 0.014 Ω cm below the transition and simultaneously the higher EPR linewidth cannot be explained by the Elliot expression. Moreover, the increase of ΔB cannot be explained by the change of Δg, as follows from figure 2. We believe that a new spin relaxation mechanism appears below the transition.

Our results disagree with earlier published EPR data [6], where $\Delta B(T)$ drops by ∼25% at 213 K and stays temperature independent down to 90 K. The corresponding signal intensity, determined as $I_{\rm epr} \sim A(\Delta B)^2$ (A is the amplitude of the first derivative of EPR absorption), drops by 50% at $T = 213$ K. This drop primarily comes from the sharp narrowing of the $\Delta B(T)$ observed in all three principal crystal orientations (a, b, c). This is surprising because at the transition these parameters behave differently: the b-parameter decreases from 33.78 Å down to 33.66 Å, the c-parameter increases from 33.92 Å up to 34.04 Å, while the a-parameter remains unchanged. One would expect different behavior of $\Delta B(T)$ along the principal axes. In our experiments the temperature behavior of the EPR amplitude shown in figure 2 exactly compensates the changes of $\Delta B(T)$, so the EPR intensity calculated by using the above expression is constant. Moreover, this conclusion is independently confirmed by the double integration EPR spectra and $\chi_{\rm p}(T)$ dependences shown in figure 3 (inset). These facts make doubtful the earlier proposed SDW model for the low-temperature magnetic state of (BEDO-TTF)$_2$ReO$_4$·H$_2$O. We incline to the more favorable approach recently applied for the description of the ordering transformation in κ-(ET)$_2$Cu[N(CN)$_2$]Br [14].

The theoretical Curie–Weiss estimates give 1.88×10^{-1} emu mol^{-1} at 2 K and 1.25×10^{-3} emu mol^{-1} at 300 K for the case where all cation-radicals contribute to the ensemble of non-interacting localized spins $S = 1/2$. The measured contribution from the local moments at 300 K is $(4.25 - 1.62) \rightarrow 2.63 \times 10^{-4}$ emu mol^{-1}, which is roughly five times less then the respective estimate. This means that the rest of the electrons contribute to the metallic state. In other words, nearly 20% of BEDO-TTF cation-radicals exist in the form of localized magnetic states.

In the current study $I_{\rm epr}(T)$ proportionally decreases with temperature. Hence, together with $n(\varepsilon_{\rm F})$ the fraction of delocalized moments decreases with switching from conducting holes to localized electrons. The total paramagnetic susceptibility, $\chi_{\rm p}(T)$, shows neither abrupt changes in the vicinity of the Me–Me′ transition nor fast growth below it. It is reasonable to interpret the behavior $\chi_{\rm p}(T)$, $14 < T < 200$ K depicted in figure 3 in terms of short-range antiferromagnetic (AFM) coupling [15]. However, this cannot be direct AFM interactions, because x-ray analysis to within 1% accuracy denies the admixture of other crystallographic phases above and below $T_{\rm c}$. The scenario of alternating metallic and insulating cation-radical layers also contradicts the smooth opposite trends in $\chi_{\rm p}(T)$ and $I_{\rm epr}(T)$.

Analyzing the $\chi_{\rm p}(T)$ behavior in the range $14 < T < 50$ K, one can estimate the effective AFM coupling constant, $|J_{\rm eff}/k| \simeq 35$ K, in the ensemble of the local moments. This value is too small for direct AFM exchange between adjacent BEDO dimers. Therefore, we suppose that local moments are scattered over the crystal volume. However, in this case their concentration is not enough for direct AFM exchange.

The EPR linewidth broadening below 203 K and unusual contribution to its angular dependences indicate the involvement of conduction electrons in the interaction between local moments. Indeed, the contribution $\sim(1 - 3\cos^2\theta)$ might be evidence in favor of in-plane

magnetic interactions [16]. Note that the anomaly appears at the magic angle $\theta = 54.7^\circ$ (see the maxima at $90^\circ \pm 54.7^\circ$ in figure 5).

Below 14 K, $\chi_p(T)$ increases, reaching 1.3×10^{-1} emu mol^{-1} at 2 K. We interpret this fact as a recovery of the paramagnetic state in the system of local moments. This value is at least 30% smaller than the maximal estimate for non-interacting $S = 1/2$ moments on each BEDO dimer. Therefore, a certain fraction of electrons still contribute to the metallic state. That is in good agreement with the metallic behavior of $\rho(T)$ with 0.003 Ω cm at 4.2 K. Note that, at $T = 14$ K, $\chi_p = 4.4 \times 10^{-4}$ emu mol^{-1}, which reveals the existing magnetic response of the metallic state.

We believe that a realistic model explaining the experimental data presented supposes localized moments $S = 1/2$ homogeneously scattered over the cation-radical layers and AFM interacting via conduction electrons (holes). It is likely that the moments are located on isolated BEDO dimers ($BEDO^{+1}$–$BEDO^{0}$) and that their concentration increases on cooling, so that short-range AFM coupled states appear below 35 K. In turn, the concentration of conducting electrons continuously decreases until the lack of them destroys the magnetically coupled states, since their presence is necessary for AFM interaction between local moments. This interpretation is also consistent with the temperature dependence of the Hall resistivity, where the unusual anomalies were observed at ∼10, 35 and 50 K [6].

We understand the phenomenon of coexistence of localized and delocalized moments and their mutual interaction in conducting BEDO-TTF layers in the framework of the inhomogeneous electronic states of the uniform quasi-electronic spectrum. This is an interesting new phenomenon which is rarely observed in organic metals.

Recently similar indications of inhomogeneous electronic states have been made in a series of EPR and resistivity measurement on $(BET\text{-}TTF)_2ReO_4$ [10]. We believe that very recent direct observation of inhomogeneous electronic states in $(ET)_2Cu[N(CN)_2]Br$ by using scanning microregion infrared reflectance spectroscopy (SMIS) also supports our interpretation [17–19].

Most reasonably, the localization in a cation-radical layer is due to the influence of non-magnetic ReO_4 anions. The hydrogen bonds between terminal ethylene groups of BEDO-TTF and ReO_4, and electric dipole moments of ReO_4 tetrahedra, induce the modulating potential on conducting BEDO-TTF layers. Since the participation of the oxygen p orbitals in the HOMO is weak, the anion layer causes only a minor effect on the band structure and the Fermi surface of $(BEDO\text{-}TTF)_2ReO_4{\cdot}H_2O$ [8]. Due to hydrogen bonding, the water molecules 'glue' pairs of tetrahedra, and long-range modulation does not occur. Instead, the fine anion rearrangement takes place. Even though the structure is homogeneous, the single H_2O molecule per unit cell is not enough for a regular polymeric 2D network. Thus, the discontinuities of the modulation field act as a certain amount of disorder. In some sense, the randomness can be considered as a 'phase break' of the modulation. Due to the Anderson localization or similar mechanisms an increasing number of local moments appear below the Me–Me′ transition. Thus, collective BEDO dimers ($BEDO^{+1/2}$–$BEDO^{+1/2}$) convert into isolated ($BEDO^{+1}$–$BEDO^{0}$) with $S = 1/2$. The localized moments can possibly arise in BEDO dimers in the vicinity of these phase irregularities.

5. Conclusion

By using EPR and SQUID methods, consistent information about spin ensembles of the quasi-2D organic metal $(BEDO\text{-}TTF)_2ReO_4{\cdot}H_2O$ was obtained. It is concluded that a subsystem of delocalized spins in the BEDO-TTF layer contributes to the EPR signal, whereas the static magnetic susceptibility, χ_p, measured by the SQUID is mainly governed

by localized spin states. The electronic phase transition Me–Me′, induced by fine structural rearrangement of ReO_4 tetrahedra, leads to the appearance of local moments, which interact antiferromagnetically at lower temperatures. It is detected by the spin-lattice relaxation of conduction electrons and the amplitude of the EPR signal. However, it is not observed in static spin susceptibility and the intensity of the EPR signal. The relative proportion between the two spin systems gradually changes with cooling. Thus, the current study provides the experimental evidence of coexisting delocalized conduction electrons and localized magnetic moments in $(BEDO\text{-}TTF)_2ReO_4{\cdot}H_2O$ and their mutual interaction.

We conclude that the layered organic metal $(BEDO\text{-}TTF)_2ReO_4{\cdot}H_2O$ possesses an inhomogeneous electronic spectrum arising below the Me–Me′ phase transition. Inhomogeneous electronic states exist in the cation layers. They are characterized by localized (local moments) and delocalized (conducting electrons) electronic states. The local moments interact via delocalized spins of conducting electrons resulting in the short-range AFM coupled states. We attribute the results obtained to a new physical phenomenon recently found in the family of metallic cation-radical salts due to their highly correlated electron system [10, 17–19].

Acknowledgments

The authors are thankful to Dr L I Buravov for resistivity data. This work was supported by the Netherlands Organization for Scientific Research grant 047.008.020, the Russian Academy of Sciences grants 24, 29 and the Russian Foundation for Basic Research through grant NSH-5859.2006.2.

References

[1] Williams J M, Ferraro J R, Thorn R J, Carlson K D, Geiser U, Wang H H, Kini A M and Whangbo M-H 1992 *Organic Superconductors (Including Fullerenes), Synthesis, Structure, Properties, and Theory* (Englewood Cliffs, NJ: Prentice-Hall)
[2] Williams J M, Schultz A S, Geiser U, Carlson K D, Kini A M, Wang H H, Kwok W-K, Whangbo M-H and Schirber J E 1991 *Science* **252** 1501
[3] Day P 1993 *Phys. Scr.* **49** 726
[4] Buravov L I, Khomenko A G, Kushch N D, Laukhin V N, Schegolev A I, Yagubskii E B, Rozenberg L P and Shibaeva R P 1992 *J. Physique* I **2** 529
[5] Kahlich S, Sommer W, Schweitzer D, Heinen I, Keller H J, Rovira C, Paradis J A and Whangbo M-H 1995 *Synth. Met.* **70** 865
[6] Kahlich S, Schweitzer D, Rovira C, Paradis J A, Whangbo M-H, Heinen I, Keller H J, Nuber B, Bele P, Brunner H and Shibaeva R P 1994 *Z. Phys.* B **94** 39
[7] Tanatar M A, Swietlik R, Kushch N D and Yagubskii E B 1997 *J. Phys.: Condens. Matter* **9** 30
[8] Khasanov S S, Narymbetov B Zh, Zorina L V, Rozenberg L P, Shibaeva R P, Kushch N D, Yagubskii E B, Rousseau R and Canadell E 1998 *Eur. Phys. J.* B **1** 419
[9] Khasanov S S, Zorina L V, Shibaeva R P, Kushch N D, Yagubskii E B, Rousseau R, Canadell E, Barrans Y, Gaultier J and Chasseau D 1999 *Synth. Met.* **103** 1853
[10] Khasanov S, Perez-Benitez A, Narymbetov B Zh, Zorina L V, Shibaeva R P, Singleton J, Klehe A, Laukhin V N, Vidal-Gancedo J, Veciana J, Canadell E and Rovira C 2002 *J. Mater. Chem.* **12** 453
[11] Wertz J E and Bolton J R 1972 *Electron Spin Resonance: Elementary Theory and Practical Applications* (New York: McGraw-Hill)
[12] Voronkova V K, Zaripov M M, Kogan V A and Yablokov Yu V 1973 *Phys. Status Solidi* b **55** 747
[13] Shvachko Yu N, Starichenko D V, Korolyov A V, Kushch N D and Yagubskii E B 2005 *Preprint* cond-mat/0506634
[14] Tanatar M, Ishiguro T, Kondo T and Saito G 2000 *Phys. Rev.* B **61** 3278
[15] Carlin R L 1986 *Magnetochemistry* (Berlin: Springer)
[16] Dumm M, Loidl A, Alavi B, Starkey K, Montgomery L and Dressel M 2000 *Phys. Rev.* B **62** 6512
[17] Sasaki T, Yoneyama N, Kobayashi N, Ikemoto Y and Kimura H 2004 *Phys. Rev. Lett.* **92** 227001
[18] Sasaki T, Yoneyama N, Suzuki A, Kobayashi N, Ikemoto Y and Kimura H 2005 *J. Phys. Soc. Japan* **74** 2351
[19] Yoneyama N, Sasaki T, Kobayashi N, Ikemoto Y and Kimura H 2005 *Phys. Rev.* B **72** 214519